COMMUNICATION

N,N'-Dimethylsquaramide as a central scaffold for anionophore design

Daniel A. McNaughton[a], Edward York[a], Tristan Rawling[a] and Philip A. Gale[a,*]

Received 00th January 20xx,
Accepted 00th January 20xx

DOI: 10.1039/x0xx00000x

The *N,*N'-dimethylation of a diphenylsquaramide induces a conformational change in the orientation of the phenyl rings. This has been exploited to create a series of bis-urea, -thiourea and -squaramide hydrogen bond donor anionophores. The compounds were shown to transport H^+/Cl^- in lipid bilayers, whereas a non-methylated analogue displayed limited transport activity. Despite their potency in transport studies, the series had a negligible impact on cancer cell viability.

Introduction

Synthetic anionophores that facilitate Cl^- transport across cell membranes have been explored for their potential anticancer activity. Studies have shown that chloride transport into cells may trigger cell death via caspase-dependent apoptosis, often coupled with a disruption of cellular pH gradients.[1] Our group and our collaborators have demonstrated that lysosomal pH disruption can also interfere with autophagy, compounding the potential cytotoxic effects.[2] Alternatively, active anion transporters that remain non-toxic towards cells can potentially treat debilitating channelopathies, such as cystic fibrosis.[3]

One effective strategy in the design of active anionophores is to append two or more convergent hydrogen bond donors to a central scaffold. For instance, *ortho*-phenylene scaffolds have proven effective in creating extremely potent bis-urea anion transporters.[4] Researchers have employed various donor motifs to create a pre-organised cavity and altered the central structure to tune the bite-angle and anion binding affinity.[5] This central group can provide additional hydrogen bond donors to the binding site or possess additional properties, such as fluorescence.[6]

Simple diarylsquaramides have emerged as a class of anionophores capable of efficient Cl^- transport.[7] These motifs typically adopt a *trans-trans* conformation upon anion complexation to enhance the involvement of both amide protons and reduce steric hindrance from the other attached groups.[7] *N,N'*-dimethylation of aryl squaramides, however, causes the molecule to preferentially adopt a *cis-cis* conformation to minimise interactions between the two *N*-methyl groups, leaving the aryl substituents in a convergent, cofacial arrangement **(Fig 1.)**.[8] Recently, Tanatini and co-workers constructed oligomers containing multiple *N,N'*-dimethylated squaramides. The species displayed *cis-cis* conformations in the solid-state, with *meta*-substituted compounds adopting helical-like structures.[9]

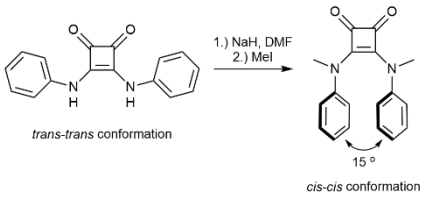

Fig 1. The effect of *N*-methylation on the preferred conformation of *N,N'*-diphenylsquaramide.

In this work, *N,N'*-dimethyl-*N,N'*-diphenylsquaramide has been employed as a central scaffold in the formation of a series of anionophores with dual hydrogen bonding groups. It was envisioned that the preferred co-facial arrangement and small dihedral angle (15°) of the phenyl groups would create an encapsulating binding cavity for a guest anion.[8] A variety of dual hydrogen bond donor motifs and electron-withdrawing -CN or -NO_2 phenyl substituents were appended to provide a range of anion binding affinities.

[a] *School of Mathematical and Physical Sciences, Faculty of Science, University of Technology Sydney, Sydney, NSW 2007, Australia. Email: Philip.gale@uts.edu.au*
† Footnotes relating to the title and/or authors should appear here.
Electronic Supplementary Information (ESI) available: [details of any supplementary information available should be included here]. See DOI: 10.1039/x0xx00000x

Results and discussion

Synthesis

The series of anionophores (**1**−**5**, Fig. 2) were synthesised via a pathway adapted from the method reported by Arimura *et al*.[9] *m*-Nitroaniline was added to a solution of 3,4-diethoxy-3-cyclobutene-1,2-dione in DMF:toluene (1:19) to afford *m*-nitrophenyl squaramide. This compound was methylated in dry DMF *via* initial priming with NaH (2.2 equiv.) for 10 min, followed by the addition of iodomethane. The mixture was stirred overnight before being poured into a solution of saturated NH_4Cl, and the precipitate was collected.

Multiple attempts at nitroaromatic reduction using Pd/C or Zn/NH_4Cl methods resulted in decomposition during the reaction process; therefore, $SnCl_2{\cdot}2H_2O$ in a mixture of HCl/EtOH at 80 ˚C was employed to yield the diamine intermediate.[10] Compounds **1**−**4** were synthesised by reacting the diamine with the appropriate iso(thio)cyanate in either dry dichloromethane or THF. Compound **5** was prepared by reacting the diamine with a 4-cyanophenyl-ethylsquarate intermediate in DMF:toluene (1:19) before evaporating the solvent and washing the precipitate with ethanol. Compound **6** was synthesised in one step following a literature procedure.[7] Full details of the synthetic procedures can be found in the supplementary information.

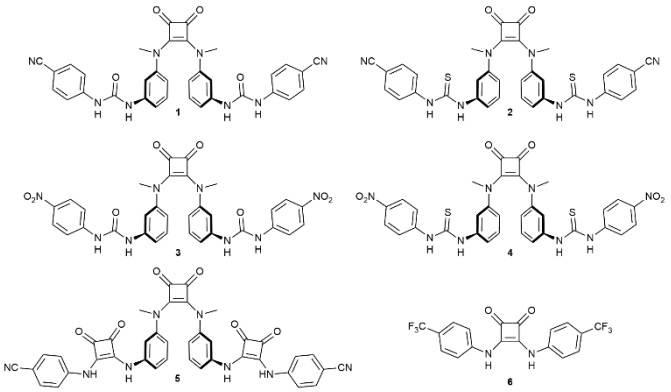

Fig. 2 The chemical structures of *N,N'*-dimethylated squaramide-centred anionophores **1**–**5**. Positive control compound **6**.

Anion binding studies

Proton NMR titration studies were undertaken to assess the Cl^- binding capabilities of compounds **1**−**5**. Experiments were completed in DMSO-d_6 with the host titrated against TBACl (0−100 equiv.). The shifts in hydrogen bond donor resonances were fitted to binding models using the Bindfit applet.[11] After examining the covariance of fit, a 1:2 binding model was preferred (a full table of results covering both binding models is available in Table S1). The results for this model are displayed in **Table 1**.

The K_{11} values for compounds **1**−**4** ranged from 158 to 463 M^{-1}, representing moderate binding towards Cl^- in competitive solvent media. Observation of the stacked NMR spectra showed that the proton resonances attributed to the ureas did not begin to plateau during the titration, even at 100 equiv. of guest. Dual hydrogen bonding scaffolds often participate in intramolecular hydrogen bonding, resulting in preorganised conformations less suited for anion binding.[4,5] To accommodate Cl^- within a convergent binding cavity, these competitive interactions must be disrupted, resulting in diminished binding affinities.

Table 1 Summary of the stability constants for the complexation of receptors **1**–**5** and Cl^- (as TBA salt) in DMSO-d_6 at 298 K.

CMPD	K_{11}[a] (M^{-1})	K_{12}[a] (M^{-1})	β_{12}[b] (M^{-2})	α[c]	F Cov_{fit}[d]
1	158	14	2.2 x 10^3	0.35	64
2	255	10	2.6 x 10^3	0.16	12
3	240	26	6.2 x 10^3	0.43	3
4	463	24	1.1 x 10^4	0.21	5
5	-[e]	-	-	-	-

[a] Errors <10 %. [b] Overall stability constant (β) is given by $\beta\ (M^{-2}) = K_{11}K_{12}$. [c] The interaction parameter (α) is calculated by multiplying K_{12} by 4 and dividing by K_{11}; a value of $\alpha < 1$ is indicative of negative cooperativity.[11] [d] The factor of covariance of fit (F Cov_{fit}) calculated by dividing Cov_{fit} 1:2 by Cov_{fit} 1:1; a value greater than 5 indicates a 1:2 binding model is favoured. [e] Could not be fit to a 1:2 binding model.

PM6 semi-empirical model ground-state equilibrium calculations were performed using Spartan '14 V1.1.4 for **4** in its ground state and in the presence of Cl^- (**Fig. S70** and **S71**). The ground state calculations reveal the presence of an intramolecular hydrogen bond between the protons of one thiourea group and the sulfur atom of the other. Facilitating this interaction is favoured over the π-π stacking of the aromatic rings adjacent to the *N*,*N*'-dimethylsquaramide. Introducing Cl^- results in a conformation rearrangement to the orientated binding mode, with aromatic π-π stacking now present. Overcoming these intramolecular thiourea interactions to adopt the binding conformation hinders effective anion coordination and is reflected in the moderate binding affinities.

The results were compared by calculating each receptor's overall binding constant (β_{12}). A slight increase in the overall binding affinity is seen between compounds **1** and **2**, where the urea groups are substituted for thioureas. However, the K_{11} value of **2** is larger, reflecting the enhanced donicity of the thiourea groups. Compound **4** possessed the highest β_{12} value, highlighting the enhancement in binding affinity facilitated by the strongly electron-withdrawing $-NO_2$ groups.

The interaction parameters (α) calculated for receptors **1**−**4** indicate strong negative cooperativity between the two binding events and that a 1:1 binding mode is preferred. This suggests that the 1:1 binding mode encompasses both hydrogen bond donor motifs, as depicted in **Fig. S71**. The approach of a second Cl^- leads each motif to bind to an individual anion, removing this cooperativity. This event is highly unfavourable, leading to low K_{12} values. Compound **5** could not be fit to a 1:2 binding model, which suggests that electronic repulsion between the two squaramide motifs inhibits a binding mode that can host two Cl^-. By comparing the 1:1 binding coefficients (**Table S1**), compound **5** (K_a = 231 M^{-1}) was shown to bind Cl^- over twice as efficiently as compound **4** (K_a = 92 M^{-1}).

The titrations were repeated in a less competitive solvent mixture of CD_3CN/2% DMSO-d_6 to elucidate more information about the binding process. Compounds **1**, **2**, and **4** were soluble in this solvent mixture, and the results are shown in **Table 2**. As expected, the apparent association constants were much larger in this solvent medium. A clear plateau in the resonance shifts attributed to the (thio)urea protons is visible after 1 equiv., before a second shift occurs between 2.5−10 equiv. This suggests that both (thio)urea groups are initially involved in a strongly coordinating convergent binding cavity before each independently binding a Cl^- at higher concentrations. The small α values, indicative of negative cooperativity, suggest that the second binding event is disfavoured.[11]

Table 2 Summary of the stability constants for the complexation of receptors **1–5** and Cl^- (as TBA salt) in CD_3CN/2% DMSO-d_6 at 298 K.

CMPD	K_{11}[a] (M^{-1})	K_{12}[a] (M^{-1})	β_{12}[b] (M^{-2})	α[c]	F Cov_{fit}[d]
1	24000	43	1.0 x 10^6	0.007	128
2	40000	28	1.1 x 10^6	0.003	56
3	-[e]	-	-	-	-
4	104000	47	4.9 x 10^6	0.002	112
5	-[e]	-	-	-	-

[a] Errors <20 %. [b] Overall stability constant (β) is given by $\beta(M^{-2}) = K_{11}K_{12}$. [c] The interaction parameter (α) is calculated by multiplying K_{12} by 4 and dividing by K_{11}; a value of $\alpha < 1$ is indicative of negative cooperativity.[11] [d] The factor of covariance of fit (F Cov_{fit}) calculated by dividing Cov_{fit} 1:2 by Cov_{fit} 1:1; a value greater than 5 indicates a 1:2 binding model is favoured. [c] Insoluble in the solvent mixture.

Similar to the results in pure DMSO-d_6, compound **4** returned the highest β_{12} value. Whilst this work was in progress, Natarajan and co-workers reported on a *N,N'*-dimethylurea receptor and examined its Cl^- recognition ability in the same solvent mixture.[12] The compound displayed a similar K_{11} = 26000 M^{-1}, but a K_{12} value which was 10-times higher (K_{12} = 550 M^{-1}). The *N,N'*-dimethyl-*N,N'*-diphenylurea scaffold has a larger dihedral angle (30°),[13] suggesting that a greater separation between the two urea motifs results in a slightly more favourable 1:2 binding mode.

Anion transport studies

Chloride/nitrate exchange assay

The anion transport ability of the compounds was initially investigated using a Cl^-/NO_3^- exchange ISE assay (results shown in Table 3). EC_{50} is the effective concentration of the transporter that gives 50% chloride release at a designated time in the experiment. The lower the EC_{50} value, the more effective the transporter. All compounds facilitated Cl^- transport at low concentrations ($EC_{50} \leq 0.33$ mol%, with respect to lipid concentration). The superior activity of thioureas **2** and **4** relative to their urea counterparts can be attributed to the greater donor acidity and lipophilicity of the thiourea groups, often resulting in enhanced anion transport due to more effective incorporation into the membrane. Compound **5** was the least active of the series, which was attributed to its poor solubility under the ISE experimental conditions (see the supplementary information for more details).

Table 3 The results of the Cl^-/NO_3^- ISE assay for receptors **1–6**.

	EC_{50}[a] (mol%)	Hill coefficient (n)	k_{ini}[b] (% s^{-1})	c log P[c]
1	0.20	0.8	1.37	3.88
2	0.06	1.2	2.51	4.55
3	0.12	0.9	0.87	4.54
4	0.03	1.3	1.61	5.26
5	0.33	1.4	0.35	4.71
6	0.06[d]	1.2	-[e]	4.58

[a] EC_{50} at 270 s, shown as receptor:lipid molar percentage. [b] Maximum initial rate calculated at a loading of 0.5 mol% by fitting efflux plot to an exponential decay function. [c] Average c log P values calculated using VCClab.[14] [d] EC_{50} value was previously reported.[2] [e] Initial rate was not reported in the previous study.

Compound **6** has been studied previously using the Cl^-/NO_3^- exchange ISE assay.[2] Its transport activity (EC_{50} = 0.06 mol%) is comparable to compound **2** and is surpassed by compound **4** (EC_{50} = 0.06 and 0.03 mol%, respectively), which indicated that the thiourea-containing anionophores might also facilitate anion transport in cellular environments. The octanol-water partition coefficients (c log P) were calculated for the series using the VCCLab ALOGPS2.1 applet.[14] This is a measure of the lipophilicity of a molecule, a key consideration in anionophore design where a degree of lipophilicity is required for molecules to partition into and pass through the hydrophobic interior of the bilipid membrane successfully. The transport activity of compounds **1**−**4** increases with increasing lipophilicity, highlighting the influence of this property on anion transport.

The Hill coefficient (n) indicates the stoichiometry of the transport event. Each receptor returned a value close to 1.0, suggesting that a 1:1 host:guest complex in the preferred convergent binding conformation facilitates Cl^- efflux across the membrane.

Cationophore coupled transport assay

Next, a cationophore-coupled assay was employed to elucidate the preferred Cl^- transport mechanism.[15] Valinomycin is a strict K^+ uniporter, meaning anion transport coupled to this cationophore occurs via an electrogenic Cl^- uniport pathway. Monensin operates as a H^+/K^+ exchanger, meaning anion transport in the presence of this species occurs as electroneutral H^+/Cl^- co-transport. Full experimental details can be found in the supplementary information. All anionophores were shown to transport H^+/Cl^- over electrogenic Cl^- transport (**Fig. 3a**). An electroneutral factor coefficient (E_{neut}) was calculated for each anionophore as a ratio of initial rate (k_{ini}) in the presence of monensin over k_{ini} with valinomycin (Table S4). Positive values between E_{neut} = 1.9–9.5 (for **5** and **3**, respectively) were calculated across the series. This means the compounds facilitate H^+/Cl^- co-transport much more effectively than chloride uniport.

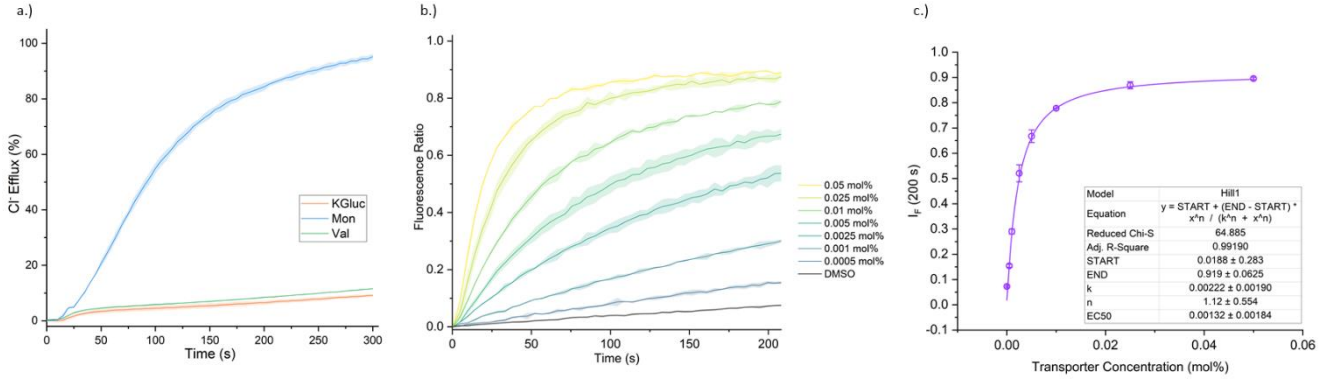

Fig. 3 a.) Chloride efflux facilitated by **4** (0.1 mol%) in the cationophore coupled assay with no cationophore (orange), in the presence of 0.1 mol% monensin (blue) and 0.1 mol% valinomycin (green). **b.)** Efflux plot of the dose-response studies for compound **4** in the NaCl HPTS assay. Each data point is the average of two repeats with error bars to show standard deviation. **c.)** Hill plot of compound **4**.

HPTS assay for HCl transport

Following mechanistic studies, the H^+/Cl^- cotransport ability of the series was measured using the HPTS assay.[16] In this assay, both the internal and external solution contain NaCl (100 mM) buffered to pH 7.0, and the internal solution contains HPTS (1 mM), a pH-sensitive fluorescent dye. An anionophore is added to the experiment, and transport is initiated via a NaOH pulse, which raises the extravesicular pH to 8.0. Transport of H^+/Cl^- out of the vesicles is tracked via changes in the emission intensities of the HPTS dye. Several concentrations of each anionophore were tested to establish a dose-response curve, and the efflux reading at 200 s was taken for each concentration and fit to the Hill equation. Initial transport rates (k_{ini}) were calculated using an exponential decay function. The efflux and Hill plots for compound **4** are shown in Fig. 3b&c, and the experimental results are shown in Table 4.

Compound **4** demonstrated the highest activity of the series, highlighting the potent combination of lipophilic thiourea donors and strongly electron-withdrawing -NO_2 groups (EC_{50} = 0.0029 mol%, or 1.3 nM. Urea-based compound **3** outperformed thiourea-containing compound **2** in this assay, contrary to the results of the ISE exchange assay. NO_2 substituents are also more lipophilic than CN groups, compounding their ability to enhance transport activity.

Table 4 The results of the NaCl HPTS assay for receptors **1–5**.

	EC_{50} [a] (mol%)	EC_{50} (nM)	Hill coefficient (*n*)	k_{ini} [b] (10^{-2} % s^{-1})
1	0.0045	4.5	1.3	4.13
2	0.0029	2.9	1.3	5.29
3	0.0023	2.3	1.1	5.14
4	0.0013	1.3	1.1	6.03
5	0.0047	4.7	1.2	2.74
6	0.0018	1.8	0.9	6.86

[a] EC_{50} at 200 s, shown as receptor:lipid molar percentage. [b] Maximum initial rate calculated at a loading of 0.05 mol% by fitting efflux plot to an exponential decay function.

Compound **5** was the least active of the series and exhibited a significantly slower initial rate (k_{ini} = 2.74 x 10^{-2} % s^{-1}). The transporters were added to the solution externally as a DMSO aliquot, meaning they must initially penetrate the hydrophilic outer membrane to facilitate transport. It is possible that the multiple hydrogen bond acceptors present in **5** (6 carbonyl oxygens) interact strongly with this hydrophilic layer, hindering progress into the membrane leaflet.

Compound **6** was tested using the HPTS NaCl assay for the first time, having been previously investigated before this assay was developed. Its transport efficiency in this assay is comparable to compounds **1**–**5**. Similarly to the Cl^-/NO_3^- exchange ISE assay, compound **4** (EC_{50} = 0.0013 mol%) outperformed compound **6** (EC_{50} = 0.0018 mol%). However, the trend in k_{ini} values is reversed, with **6** facilitating the fastest rate of Cl^- transport. This is likely related to the efficiency with which compound **6** can permeate into the membrane, aided by its low molecular weight and relative structural simplicity.

Compound **7** (**Fig. 4**) was synthesised to explore the importance of the *N,N'*-dimethylation step in creating a functioning anionophore. This novel species is analogous to compound **4**, the most potent anionophore of the series; however, it differs by the central squaramide scaffold remaining unmethylated. This provides an additional hydrogen bond donor capable of anion binding but removes the preference for a cofacial *cis-cis* conformation.

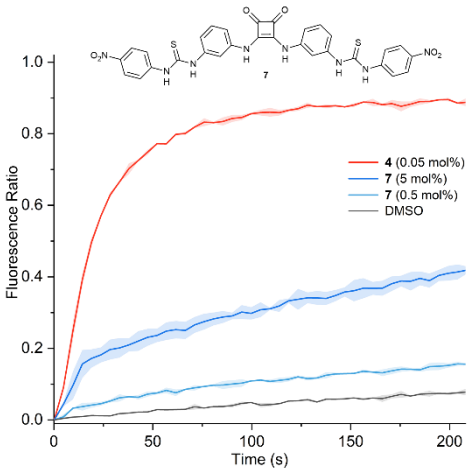

Figure 4. The structure of compound **7** and efflux plot of its transport activity in the NaCl HPTS assay (at 0.5 mol% and 5 mol% loading) compared to compound **4** (at 0.05 mol% loading).

The Cl^- transport ability of compound **7** was tested using the HPTS NaCl assay and compared to compound **4** (**Fig. 4**). Compound **7** exhibited significantly lower activity than its methylated analogue, resulting in a reduced H^+/Cl^- efflux rate at a concentration 100-fold higher. These results highlight how a simple chemical transformation to the central scaffold can lead to vastly different anionophoric capabilities. It was demonstrated by Valkenier and co-workers that compounds with two distal anion binding sites exhibit poorer anion transport, as any donor groups not involved in anion coordination will interact detrimentally with phospholipid head groups.[17] It is likely that **7** is unable to form a convergent binding site in a *trans-trans* conformation, meaning Cl^- transport is negatively influenced by head-group interactions.

Anion transport selectivity studies

The propensity of compound **3**–**6** to transport other anions selectively over Cl^- was examined using the 'anion gradient' assay developed by Wu and Gale.[18] These compounds represent the four binding site shapes explored in this work. Vesicles were prepared with the same internal conditions as that of the HPTS NaCl assay; however, in this experiment, the vesicles are suspended in external solutions of NaX (100 mM, $X^- = Cl^-$, Br^-, I^-, NO_3^- or ClO_4^-) buffered to pH 7.0. A base pulse does not initiate transport; instead, an aliquot of anionophore in DMSO (5 μL) is added at $t = 0$ s. If HCl is transported out of the vesicles quicker than HX is transported inside, then the anionophore is Cl^- selective and the vesicles will become basified. If HX transport is quicker than HCl, the vesicles will become acidified. To track this change, the fluorescence ratios are converted into pH values. The different anions can be compared by considering the maximum ΔpH values (before the pH begins to return to equilibrium), creating a selectivity sequence. The results, including a DMSO control, can be viewed in the supplementary information (**Fig. S95**–**99**).

Compounds **3** and **6** have similar selectivity sequences of $Cl^- < Br^- \leq NO_3^- < I^- < ClO_4^-$. This follows the Hofmeister series, where more hydrophobic anions are transported more effectively as they can be dehydrated more efficiently. The binding site of compound **6** exhibits no size-selectivity, meaning anion hydrophobicity is the main determining factor. It is likely that the small steric bulk of the urea motifs of compound **3** also means larger anions are readily accommodated.

The selectivity of compound **4** (**Fig. S96**) followed the sequence $Cl^- < ClO_4^- < Br^- < NO_3^- < I^-$. The trend in halide selectivity still follows that of hydrophobicity, but the preference for oxoanions NO_3^- and ClO_4^- is diminished. This is likely due to a convergent binding site which is a better match for simple spherical anions over those with more complex geometries. This is likely a consequence of the bulky sulfur atoms of the thioureas, which limit manipulation of the binding site to host larger guests. Compound **5** is selective for Cl^- over both oxoanions, returning the sequence $ClO_4^- < NO_3^- < Cl^- < Br^- < I^-$. The squaramide donors create an even more convergent binding site, further limiting the recognition of complex geometries.

Cytotoxicity studies

To assess the anticancer activity of compounds **1**–**7,** their capacity to reduce the viability of two cancer cell lines (MDA-MB-231 and A549) was assessed using the 3-(4,5-dimethylthiazol-2-yl)-5-(3-carboxymethoxyphenyl)-2-(4-sulfophenyl)-2H-tetrazolium MTS assay. Compound **6**, which has previously reported cytotoxic activity, was employed as a positive control.[2] Compound **3** was not tested due to solubility issues in the cell media.

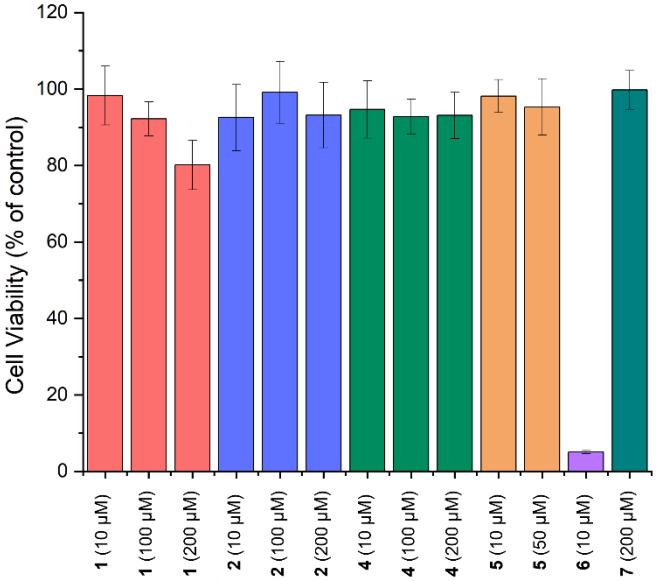

Figure 5. The % of viable A549 cells as a function of formazan absorbance (λabs = 490 nm) in the MTS assay after treatment with compounds 1–7 for 72 h. Results were repeated in triplicate across three 96-well plates, with error bars representing the SEM of the readings. The data was normalised to DMSO vehicle control.

The results for the A549 cell line are displayed in **Fig 5**. Interestingly, compounds **1**–**5** did not produce statistically significant reductions in the viability of either cell line at concentrations up to 200 μM despite their demonstrated anion transport efficacy in vesicular studies. Compound **7** was also non-toxic, while compound **6** (10 μM) reduced the viability of both cell lines to below 10 %. This could result from poor aqueous solubility or processes within the cell that destroy the anionophores before transport can occur. However, the results echo those reported by Davis and co-workers, wherein a decalin bis-urea compound was shown to be non-toxic towards epithelial cell lines whilst still facilitating efficient Cl^- transport.[19] Other strict H^+/Cl^- co-transport has been associated with anticancer and antimicrobial activity, suggesting that factors beyond their ability to mediate anion transport are limiting the effectiveness of compounds **1**–**5**.[1, 20, 21]

Experimental

General experimental methods

Deionised water was collected from a Merck Millipore Milli-Q™ reference ultrapure water purification system. The nuclear magnetic resonance (NMR) spectra were recorded at 300 K using

a Bruker AVIII 500 or Bruker Avance DPX 400 spectrometer. ^{1}H and ^{13}C NMR spectra were recorded at the indicated frequency and calibrated to the residual DMSO-d6 solvent peak (δ = 2.50 ppm and δ = 39.52 ppm, respectively). The resonances are reported as chemical shifts in ppm, multiplicity, coupling constant in Hz, and by their relative integral. Melting points were recorded using a Stuart Automatic Melting Point SMP50, and data were reported as a range (°C). Low-resolution mass spectrometry was performed with a Bruker amaZon SL mass spectrometer using electrospray ionisation. High-resolution mass spectra were recorded on a Bruker Apex II Fourier Transform Ion Cyclotron Resonance (FTICR) mass spectrometer with a 7.0 T magnet, fitted with an off-axis analytic electrospray source with quadrupole mass analyser and are reported as m/z (relative intensity).

To prepare the vesicles, a chloroform solution of POPC (37.5 mM, 4 mL) was transferred to a pre-weighed round-bottom flask, and the solvent was removed using a rotary evaporator. The pressure was lowered slowly to ensure the formation of a smooth lipid film. Subsequently, the film was dried in vacuo for 4–24 h, and the mass of lipid was recorded. The lipids were rehydrated with 4 mL of the respective internal solution (this number should correspond to the volume of POPC solution used initially) and vortexed until all lipids were removed from the sides of the flask and were suspended in solution. The lipids were subjected to 9 freeze-thaw cycles by freezing using a dry ice/acetone bath and thawing in lukewarm water. Following this, the vesicles were left to rest at room temperature for 30 min. The lipids were extruded through a 200 nm polycarbonate membrane 25 times to form monodisperse vesicles. Only 1 mL of solution was extruded at a time before being collected. Finally, any residual unencapsulated salt from the internal solution was either removed via dialysis for 12 h in the desired external solution or through size exclusion using a B19 column packed with hydrated G-25 Sephadex®, which had been pre-saturated with the respective external solution. The lipid suspensions were diluted with the external solution to afford a stock solution (10 mL) of a known concentration. The ISE assays were conducted using a Fisherbrand™ Accumet™ Chloride Combination Electrode, and the HPTS transport fluorescence data was recorded on an Agilent Cary Eclipse Fluorescence Spectrophotometer.

Human MDA-MB-231 breast cancer cells and A549 pulmonary epithelial cells (ATCC) were cultured in Dulbecco's Modified Eagle Medium containing 1% (v/v) penicillin/streptomycin (Merck, Darmstadt, Germany) and 10% (v/v) foetal bovine serum (Thermo Fisher Scientific, Waltham, MA, USA). Cells were cultured at 37 °C in a humidified atmosphere of 5% CO2 and harvested at 80–90% confluency using trypsin/EDTA after washing with Dulbecco's phosphate-buffered saline (dPBS, Merck). Test compounds were administered to cells using a DMSO vehicle (to a final concentration containing 1% DMSO v/v) and were compared against cells treated with DMSO alone (vehicle-only control). MDA-MB-231 cells were seeded in triplicate in 96-well plates (density of 3.5 x 103 cells per well) in complete media and incubated for 24 h. Separately, various concentrations of the compounds to be tested were prepared in complete media (5 µL of compound in DMSO to 995 µL of media, 200−10 µM). After removing the well media, the cells were treated with DMSO:media solutions and incubated for an additional 72 h. Subsequently, the DMSO:media solutions were replaced with untreated media and incubated with CellTiter MTS 96 Aqueous MTS Reagent Powder (Promega) and phenazine ethosulfate (Sigma Aldrich) under dark conditions for approx. 3 h. Cell viability was measured by monitoring the conversion of MTS to formazan via dehydrogenase enzymes in metabolically active cells. The absorbance at 490 nm (the absorbance wavelength of formazan) for each well was measured using a Tecan Infinite M1000 Pro plate reader (CellTiter 96 Aqueous Non-Radioactive Cell Proliferation Assay, Promega). The procedure was repeated three times to give nine readings for each concentration.

***N*-(3-nitrophenyl)squaramide (8)**. *m*-nitroaniline (2000 mg, 14.5 mmol) and zinc trifluoromethanesulfonate (877 mg, 2.42 mmol) were dissolved in a mixture of toluene (9.5 mL) and DMF (0.5 mL) before 3,4-diethoxy-3-cyclobutene-1,2-dione (0.65 mL, 4.35 mmol) was added dropwise to the solution. This was heated to 100 °C and left to stir for 3 d. A precipitate formed, which was collected upon cooling and filtered. The precipitate was subsequently washed with DCM (2 x 35 mL) and MeOH (2 x 35 mL) to yield a bright yellow solid (1400 mg, 3.95 mmol, 91%).

^{1}H NMR (500 MHz, DMSO-d_6) δ ppm 10.36 (2 H, b), 8.37 (2 H, s), 7.90 (2 H, d, J 8.1), 7.79 (2 H, d, J 8.1), 7.64 (2 H, t, J 8.2).

LR-MS (ESI$^+$) *m/z* 377.1 [M+Na]$^+$, (ESI$^-$) *m/z* 353.03 [M−H]$^-$.

***N*-(3-nitrophenyl)-*N*'-(methyl)squaramide (9)**. Sodium hydride (60 %, 200 mg, 5 mmol, washed twice with hexane) was suspended in dry DMF (3 mL). This was added dropwise and slowly to a solution of compound **8** (800 mg, 2.26 mmol) dissolved in dry DMF (10 mL), which had been cooled to 0 °C. This was allowed to warm to room temperature and stirred for 10 min before iodomethane (2.5 mL) was added dropwise. The reaction mixture was stirred at RT for 1 d before being poured into an aqueous solution saturated with ammonium chloride. The precipitate was collected by vacuum filtration and washed with methanol to yield compound **9** (580 mg, 1.51 mmol, 67%).

^{1}H NMR (400 MHz, DMSO-d_6) δ ppm 7.62 (2 H, dd, J 6.4, J 2.4), 7.56 (2 H, s), 7.30 (4 H, m), 3.69 (6 H, s).

LR-MS (ESI$^+$) *m/z* 405.07 [M+Na]$^+$.

***N*-(3-aminophenyl)-*N*'-(methyl)squaramide (10)**. Tin(II) chloride dihydrate (5 g, 22 mmol) was added to conc. HCl (32%, 15 ml) and left to stir for 10 min. Next, compound **9** (800 mg, 2.09 mmol) was added portion-wise, followed by 5 mL of conc. HCl to wash compound off the sides. This was stirred at 50 °C for 1 h before 24 mL of EtOH was added, and the temperature increased to 80 °C. The mixture was stirred for 3 h before the EtOH was removed with a stream of nitrogen to evaporate the EtOH. The remaining solution was poured into 20 mL of water and neutralised using NaOH solution. The resultant precipitate, which contained a large portion of tin hydroxide, was collected on celite via vacuum filtration. This precipitate cake was extracted with EtOAc to give a light green solution, which was then evaporated to leave compound **10** as a light yellow powder. The aqueous layer was also green and was evaporated under

nitrogen to also leave a yellow powder (500 mg, 1.55 mmol, 74%).

^{1}H NMR (400 MHz, DMSO-d6) δ ppm 6.76 (2 H, t, J 7.85), 6.20 (2 H, dd, J 8.15, J 1.89), 6.11 (4 H, m), 5.01 (5 H, s), 3.37 (6 H, s).

LR-MS (ESI^+) *m/z* 323.18 $[M+H]^+$, 345.12 $[M+Na]^+$, (ESI^-) *m/z* 321.13 $[M-H]^-$.

***N*-(4-cyanophenylurea)-*N'*-(methyl)squaramide (1)**. Compound **10** (65 mg, 0.2 mmol) was dissolved in dry DCM (6 mL) and stirred for 5 min. Next, 4-cyanophenyl isocyanate (72 mg, 0.5 mmol) was added portion-wise over 5 min, leaving a brown solution stirred at RT overnight. A precipitate formed; however, the solvent was evaporated without filtration, and the solids were taken up in 10 mL of MeOH. This was sonicated, filtered, and dried to yield a crystalline yellow solid (70 mg, 0.11 mmol, 57%).

MP = 223−226 °C.

^{1}H NMR (400 MHz, DMSO-d_6) δ ppm 8.26 (2 H, s), 7.91 (2 H, s), 6.84 (4 H, m), 6.77 (4 H, m), 6.29 (2H, t, J 2.14), 6.10 (2 H, t, J 8.09), 5.97 (2 H, ddd, J 8.22, 2.10, 0.91), 5.68 (2 H, ddd, J 8.09, 2.30, 0.91), 2.80 (6 H, s); **^{13}C NMR** (101 MHz, DMSO-d_6) δ ppm 186.7, 167.6, 152.3, 144.5, 143.7, 139.9, 133.7, 129.3, 119.7, 118.5, 114.5, 114.2, 110.9, 103.7, 38.3.

LR-MS (ESI^-) *m/z* 609.23 $[M-H]^-$; **HR-MS** (ESI^+) calcd for $C_{34}H_{26}N_8NaO_4$ $[M+Na]^+$: 633.19692, found *m/z* 633.19597.

***N*-(4-cyanophenylthiourea)-N'-(methyl)squaramide (2).** Compound **10** (80 mg, 0.25 mmol) was dissolved in dry THF (5 mL) and stirred for 2 min. Next, 4-cyanophenyl isothiocyanate (100 mg, 0.62 mmol) was dissolved in dry THF (1 mL) and added dropwise. After 1 h, the solution had turned from orange to dark brown and was left to stir overnight at RT. Following this, an additional portion of 4-cyanophenyl isothiocyanate (50 mg) was added to the reaction, which was then heated to 45 °C for 6 h. The reaction was tracked to completion via TLC, following which the solvent was evaporated and the solids washed with diethyl ether (15 mL) and ethyl acetate (5 mL) to yield a light green solid (81 mg, 0.13 mmol, 50%).

MP = 166−169 °C.

^{1}H NMR (400 MHz, DMSO-d_6) δ ppm 10.21 (1H, s), 10.05 (2 H, s), 7.75 (8 H, q, J 8.7), 7.21 (2 H, s), 7.04 (4 H, dd, J 14.04, J 6.33), 6.66 (2 H, d, J 7.65), 3.53 (6H, s); **^{13}C NMR** (101 MHz, DMSO-d_6) δ ppm 186.7, 179.2, 167.8, 144.4, 143.2, 139.7, 133.2, 129.1, 122.7, 119.8, 119.5, 117.6, 116.2, 105.8, 38.9.

LR-MS (ESI^-) *m/z* 313.89 $[M-H]^-$; **HR-MS** (ESI^+) calcd for $C_{34}H_{25}N_8O_2S_2$ $[M-H]^-$: 641.15474, found *m/z* 641.15530.

***N*-(4-nitrophenylurea)-*N'*-(methyl)squaramide (3).** Compound **10** (80 mg, 0.25 mmol) was dissolved in dry THF (4 mL) and stirred for 2 min. Next, 4-nitrophenyl isocyanate (102 mg, 0.62 mmol) was suspended in dry THF (2 mL) and added dropwise. The solution was heated to 50 oC, leading to the immediate precipitation of a bright yellow solid, and left to stir overnight at RT. The reaction was tracked to completion via TLC, after which the solvent was evaporated, and the solids were subjected to hot filtration in MeCN. Collection of the solids and drying yielded a bright yellow solid (113 mg, 0.17 mmol, 70%).

MP = 219−222 °C.

^{1}H NMR (400 MHz, DMSO-d_6) δ ppm 9.34 (2 H, s), 8.81 (2 H, s), 8.07 (4 H, d, J 8.7), 7.62 (4 H, d, J 8.8), 7.10 (2 H, s), 6.92 (2 H, d, J 8.0), 6.85 (2 H, d, J 8.3), 6.51 (2 H, d, 8.0), 3.65 (6 H, s); **^{13}C NMR** (101 MHz, DMSO-d_6) δ ppm 186.8, 167.5, 152.1, 146.7, 143.8, 141.3, 139.8, 129.3, 125.4, 117.8, 114.6, 114.4, 111.0, 38.4.

LR-MS (ESI^+) *m/z* 673.16 $[M+Na]^+$, (ESI^-) *m/z* 649.24 $(M-H)^-$; **HR-MS** (ESI^+) calcd for $C_{32}H_{26}N_8NaO_8$ $[M+Na]^+$: 674.17994, found *m/z* 674.18034.

***N*-(4-nitrophenylthiourea)-*N'*-(methyl)squaramide (4).** Compound **10** (80 mg, 0.25 mmol) was dissolved in dry THF (4 mL) and stirred for 2 min. Next, 4-nitrophenyl isothiocyanate (112 mg, 0.62 mmol) was dissolved in dry THF (2 mL) and added dropwise. The solution was left to stir overnight at RT. The reaction had not reached completion overnight. Therefore, another portion of 4-nitrophenyl isothiocyanate (50 mg) was added. Following completion tracked by TLC, the solvent was evaporated, and the remaining solids were washed with 40 mL of ether. Collection of the solids and drying yielded a dark green solid (135 mg, 0.20 mmol, 79%).

MP = 150−153 °C.

^{1}H NMR (400 MHz, DMSO-d_6) δ ppm 10.47 (2 H, s), 10.25 (2 H, s), 8.18 (4 H, d, J 8.8), 7.82 (4 H, d, J 9.0), 7.24 (2 H, d, J 2.18), 7.05 (4 H, dt, J 15.8, 8.1), 6.67 (2 H, m), 3.55 (6 H, s) **^{13}C NMR** (101 MHz, DMSO-d_6) δ ppm 183.4, 179.6, 170.2, 163.2, 145.2, 141.5, 125.6, 117.7, 53.1, 42.4, 35.2, 28.9.

LR-MS (ESI^+) *m/z* 705.10 $[M+Na]^+$, (ESI^-) *m/z* 681.23 $(M-H)^-$; **HR-MS** (ESI^+) calcd for $C_{32}H_{26}N_8NaO_6S_2$ $[M+Na]^+$: 705.13089, found *m/z* 705.13048.

***N*-(4-cyanophenyl)-*N'*-(methyl)squaramide (11).** *p*-Cyanoaniline (500 mg, 4.23 mmol) and zinc trifluoromethanesulfonate (200 mg, 1.05 mmol) were dissolved in EtOH (25 mL) before 3,4-diethoxy-3-cyclobutene-1,2-dione (0.63 mL, 4.23 mmol) was added dropwise to the solution. The mixture was stirred at Rrt overnight, resulting in the formation of a yellow precipitate. This was collected, washed with EtOH and dried to yield a bright yellow product (720 mg, 2.98 mmol, 70 %)

^{1}H NMR (400 MHz, DMSO-d_6) δ ppm 11.08 (1 H, s), 7.83 (2 H, s), 7.58 (2 H, s), 4.82 (2 H, s), 1.46 (3 H, s)

LR-MS (ESI^+) *m/z* 265.05 $[M+Na]^+$, (ESI^-) *m/z* 241.03 $(M-H)^-$.

***N*-(4-cyanophenylsquaramide)-*N'*-(methyl)squaramide (5).** Compound **10** (80 mg, 0.25 mmol) and zinc trifluoromethanesulfonate (272 mg, 0.75 mmol) were dissolved in toluene (5.7 mL) and DMF (0.3 mL). Compound **11** (182 mg, 0.75 mmol) was added portion-wise, and the solution was stirred at reflux for 2 d. The solvent was evaporated, and ethanol was added to the residue. The precipitates were collected via vacuum filtration and dried to yield compound **5** as a brown solid (90 mg, 0.13 mmol, 50%).

MP = +250 °C.

^{1}H NMR (400 MHz, DMSO-d_6) δ ppm 10.07 (2 H, s), 9.84 (2 H, s), 7.82 (4 H, d, J 8.6), 7.59 (4 H, d, J 8.4), 7.17 (2 H, s), 6.99 (2 H, t, J 8.0), 6.83 (2 H, d, J 7.6), 6.61 (2 H, d, J 7.5), 3.65 (6 H, s) **^{13}C NMR** (101 MHz, DMSO-d_6) δ ppm 186.9, 182.5, 181.3,

167.5, 166.4, 165.4, 144.6, 143.0, 139.1, 134.2, 130.2, 119.0, 117.8, 115.8, 114.4, 111.0, 105.2, 38.5.

LR-MS (ESI^+) *m/z* 737.15 $[M+Na]^+$, (ESI^-) *m/z* 713.28 $(M-H)^-$; **HR-MS** (ESI^+) calcd for $C_{40}H_{25}N_8O_6$ $[M-H]^-$: 713.19025, found *m/z* 713.19094.

***N,N'*-((4-trifluoromethyl)phenyl)squaramide (6).** 3-Ethoxy-4((4-trifluoromethyl)amino)cyclobutene-1,2-dione (300 mg, 1.05 mmol) and zinc trifluoromethanesulfonate (350 mg, 0.875 mmol) were dissolved in EtOH (10 mL) before (4-trifluoromethyl)aniline (0.15 mL, 1.05 mmol) was added dropwise to the solution. This was stirred at RT for 2 d. A precipitate formed, which was collected upon cooling and filtered. The precipitate was washed with cold EtOH to yield a light yellow solid (380 mg, 0.95 mmol, 90%).

^{1}H NMR (400 MHz, DMSO-d_6) δ ppm 10.24 (2 H, s), 7.73 (4 H, d, J 8.5), 7.63 (2 H, d, J 8.5).

LR-MS (ESI^+) *m/z* 423.04 $[M+Na]^+$, (ESI^-) *m/z* 399.05 $(M-H)^-$.

***N,N'*-(3-aminophenyl)squaramide (12).** *m*-Phenylenediamine (1000 mg, 9.26 mmol) and zinc trifluoromethanesulfonate (1500 mg, 4.21 mmol) were dissolved in EtOH (15 mL) before 3,4-diethoxy-3-cyclobutene-1,2-dione (0.6 mL, 4.21 mmol) was added dropwise to the solution. This was stirred at RT for 2 d. A precipitate formed, which was collected upon cooling and filtered. The residue was purified using column chromatography in an eluent mixture of 10% MeOH/1% TEA/DCM to yield a beige solid (843 mg, 2.38 mmol, 57%).

MP = 205−208 °C.

^{1}H NMR (400 MHz, DMSO-d_6) δ ppm 9.62 (2 H, s), 6.99 (2 H, t, J 8.0), 6.76 (2 H, dd, J 7.9, 2.2), 6.60 (2 H, t, J 2.2), 6.29 (2 H, dd, J 8.0, 2.0), 5.21 (4 H, s); **^{13}C NMR** (101 MHz, DMSO-d_6) δ ppm 181.7, 166.0, 150.1, 139.7, 130.2, 109.9, 106.6, 104.0.

LR-MS (ESI^+) *m/z* 317.12 $[M+Na]^+$, (ESI^-) *m/z* 293.11 $(M-H)^-$; **HR-MS** (ESI^+) calcd for $C_{16}H_{13}N_4O_2$ $[M-H]^-$: 293.10440, found *m/z* 293.10422.

***N,N'*-(4-nitrophenylthiourea)-squaramide (7).** Compound **12** (70 mg, 0.24 mmol) was suspended in dry MeCN (5 mL) and DMF (0.25 mL). 4-nitrophenyl isothiocyanate (107 mg, 0.6 mmol) was dissolved in dry MeCN (2 mL) and added dropwise to the solution, which was stirred under argon at RT for 2 d. A yellow precipitate was collected by filtration and washed with ether and DCM to yield the desired compound as a light brown solid (91 mg, 0.14 mmol, 56%).

MP = 162−164 °C.

^{1}H NMR (400 MHz, DMSO-d_6) δ ppm 10.48 (2 H, s), 10.43 (2 H, s) 10.03 (2 H, s), 8.21 (4 H, d, J 9.0), 7.87 (4 H, d, J 9.1), 7.71 (2 H, d, J 2.2), 7.40 (4H, m), 7.18 (2 H, d, 7.8); **^{13}C NMR** (101 MHz, DMSO-d_6) δ ppm 182.0, 179.5, 166.1, 146.7, 142.9, 140.4, 139.2, 130.1, 124.8, 122.3, 118.8, 115.6, 113.8.

LR-MS ((ESI^-) *m/z* 653.19 $(M-H)^-$; **HR-MS** (ESI^+) calcd for $C_{30}H_{21}N_8O_6S_2$ $[M-H]^-$: 653.10310, found *m/z* 653.10333.

Conclusions

We have prepared a new family of anionophores based on a central *N,N'*-dimethylated squaramide scaffold. Extensive anion binding and transport studies revealed compound **4** to be the most efficient anionophore of the series, functioning as a strict H^+/Cl^- co-transporter. It outperformed compound **6**, previously reported for its efficient cellular Cl^- transport, in both ISE- and HPTS-based assays. Studies with compound **7** revealed how a simple chemical transformation can amplify into a large conformational change, resulting in profound differences in transport activity. Anion selectivity studies highlighted how different hydrogen bond motifs can create more size-selective binding sites, promoting Cl^- over oxoanions with more complex geometries. Compounds **1**−5 were found not to reduce the viability of cancer cells despite their transport efficiency being confirmed in other studies. This indicates that H^+/Cl^- co-transport in vesicular experiments does not necessarily translate to cytotoxicity, and the influence of other factors must be considered.

Author Contributions

D.A.M conducted the synthesis, NMR binding, anion and transport and cell studies. The latter was completed with training and supervision from E.Y., with supplies and materials provided by T. R. The manuscript was written by D. A. M., with T. R. and P. A. G. providing consultation and editing. P. A. G. directed the research.

Conflicts of interest

There are no conflicts to declare.

Acknowledgements

D. A. M, E. Y., T. R., and P. A. G. acknowledge and pay respect to the Gadigal people of the Eora Nation, the traditional owners of the land on which we research, teach, and collaborate at UTS. P. A. G. thanks the Australian Research Council (DP200100453) and UTS for funding.

Notes and references

1 (*a*) B.D. de Greñu, P. I. Hernández, M. Espona, D.Quiñonero, M. E. Light, T. Torroba, R. Pérez-Tomás and R. Quesada, *Eur. J. Chem.*, 2011, **17**, 14074-14083; (*b*) S. Ko, S. K. Kim, A. Share, V. M. Lynch, J. Park, W. Namkung, W. Van Rossom, N. Busschaert, P. A. Gale, J. L. Sessler and I. Shin, *Nat. Chem.*, 2014, **6**, 885-892; (*c*) X.-H. Yu, X.-Q. Hong and W.-H. Chen, *Org. Biomol. Chem.*, 2019, **17**, 1558-1571; (*d*) A. Mondal, J. A. Malla, H. Paithankar, S. Sharma, J. Chugh, and P. Talukdar, *Org. Lett.*, 2021, **23**, 6131-6136.

2 N. Busschaert, S. Park, K. Baek, Y. P. Choi, J. Park, E. N. W. Howe, J. R. Hiscock, L. E. Karagiannidis, I. Marques, V. Félix, W. Namkung, J. L. Sessler, P. A. Gale and I. Shin, *Nat. Chem.*, 2017, **9**, 667-675.

3 (*a*) B. Shen, X. Li, F. Wang, X. Yao and D. Yang, *PloS One*, 2012, **7**, e34694; (*b*) R. Quesada and R. Dutzler, *J. Cyst. Fibrosis,* 2020, **19**, 37-41.

4 S. J. Moore, C. J. E. Haynes, J. González, J. L. Sutton, S. J. Brooks, M. E. Light, J. Herniman, G. J. Langley, V. Soto-

Cerrato, R. Pérez-Tomás, I. Marques, P. J. Costa, V. Félix and P. A. Gale, *Chem. Sci.*, 2013, **4**, 103-117.
5 (a) S. Hussain, P. R. Brotherhood, L. W. Judd and A. P. Davis, *J. Am. Chem. Soc.*, 2011, **133**, 1614-1617; (*b*) T. G. Johnson, A. Docker, A. Sadeghi-Kelishadia and M. J. Langton, *Chem. Sci.* 2023, **14**, 5006-5013; (*c*) W. G. Ryder, E. G. Wu, L. Chen, M. Fares, D. A. McNaughton, K. Tran, C. Yu, and P. A. Gale, *Org. Chem. Front.*, 2024, Advance article, DOI: 10.1039/D3QO01956J
6 (*a*) C. M. Dias, H. Valkenier and A. P. Davis, *Chem. Eur. J.*, 2018, **24**, 6262-6268; (*b*) M. Fares, X. Wu, D. A. McNaughton, A. M. Gilchrist, W. Lewis, P. A. Keller, A. Arias-Betancur, P. Fontova, R. Pérez-Tomás and P. A. Gale, *Org. Biomol. Chem.*, 2023, **21**, 2509-2515.
7 (*a*) N. Busschaert, I. L. Kirby, S. Young, S. J. Coles, P. N. Horton, M. E. Light and P A. Gale, *Angew. Chem.*, 2012, **124**, 4502-4506; (*b*) G. Picci, I. Carreira-Barral, D. Alonso-Carrillo, C. Busonera, J. Milia, R. Quesada and C. Caltagirone, *Org. Biomol. Chem.*, 2022, **20**, 7981.
8 R. S. Muthyala, G. Subramaniam and L. Todaro, *Org. Lett.*, 2004, **6**, 4663-4665.
9 M. Arimura, K. Tanaka, M. Kanda, K. Urushibara, S. Fujii, K. Katagiri, I. Azumaya, H. Kagechika, and A. Tanatani, *ChemPlusChem*, 2021, **86**, 198.
10 F. D. Bellamy and K. Ou, *Tetrahedron Lett.*, 1984, **25**, 839-842.
11 (*a*) D. B. Hibbert and P. Thordarson, *Chem. Commun.*, 2016, **52**, 12792–12805; (*b*) http://supramolecular.org
12 R. Biswas, K. Samanta, S. Ghorai, S. Maji, and R. Natarajan, *ACS Omega,* 2023, **8**, 19625-19631.
13 A. Tanatani, H. Kagechika, I. Azumaya, R. Fukutomi, Y. Ito, K. Yamaguchi, and K. Shudo, *Tetahedron Lett.*, 1997, **38**, 4425-4428.
14 (*a*) I. V. Tetko and V. Y. Tanchuk, ALOGPS 2.1 (http://www.vcclab.org) is a free online program to predict log P and log S of chemical compounds. (*b*) I. V. Tetko and V. Y. Tanchuk, *J. Chem. Inf. Comput. Sci.*, 2002, **42**, 1136-1145.
15 X. Wu, E. N. W. Howe, and P. A. Gale, *Acc. Chem. Res.* 2018, **51**, 1870-1879.
16 A. M. Gilchrist, P. Wang, I. Carreira-Barral, D. Alonso-Carillo, X. Wu, R. Quesada and P. A. Gale, Supramol. Chem., 2021, **33** (7), 325-344.
17 L. Martínez-Crespo, L. Halgreen, M. Soares, I. Marques, V. Félix and H. Valkenier, *Org. Biomol. Chem.*, 2021, **19**, 8324-8337.
18 X. Wu and P. A. Gale, *Chem. Commun.*, 2021, **57**, 3979-3982.
19 H. Li, H. Valkenier, L. W. Judd, P. R. Brotherhood, S. Hussain, J. A. Cooper, O. Jurček, H. A. Sparkes, D. N. Sheppard, and A. P. Davis, *Nature Chem.*, 2016, **8**, 24-32.
20 (*a*) S. Hussain, P. R. Brotherhood, L. W. Judd, and A. P. Davis, *J. Am. Chem. Soc.*, 2011, **133** (6), 1614-1617 (*b*) H. Valkenier, L. W. Judd, H. Li, S. Hussain, D. N. Sheppard, and A. P. Davis, *J. Am. Chem. Soc.*, 2014, **136**, 12507-12512.
21 (*a*) L. E. Brennan, L. K. Kumawat, M. E. Piatek, A. J. Kinross, D. A. McNaughton, L. Marchetti, C. Geraghty, C. Wynne, H. Tong, O. N. Cavanagh, F. O'Sullivan, C. S. Hawes, P. A. Gale, K. Kavanagh and R. B. P. Elmes, *Chem*, 2023, **9**, 3138-3158. (*b*) A. Mondal, M. Siwach, M. Ahmad, S. K. Radhakrishnan, and P. Talukdar, *ACS Infect. Dis.*, 2024, **10**, 371-376.